ELSEVIER

Biochimica et Biophysica Acta 1509 (2000) 485–495

BIOCHIMICA ET BIOPHYSICA ACTA
BBA

www.elsevier.com/locate/bba

Discovery of a novel channel-forming protein in the cell wall of the non-pathogenic *Nocardia corynebacteroides*

Franziska G. Rieß *, Roland Benz

Lehrstuhl für Biotechnologie, Biozentrum der Universität Würzburg, Am Hubland, D-97074 Würzburg, Germany

Received 7 July 2000; received in revised form 14 August 2000; accepted 14 September 2000

Abstract

Detergent extracts of whole cells of the Gram-positive, non-pathogenic, strictly aerobic bacterium *Nocardia corynebacteroides* contain channel-forming activity. The protein responsible for channel formation was identified using lipid bilayer experiments. It was purified to homogeneity and had an apparent molecular mass of about 134 kDa on SDS–PAGE when it was solubilized at 40°C. When the 134 kDa protein was heated to 100°C for 10 min in sample buffer, it dissociated into subunits with a molecular mass of about 23 kDa and focused at p*I* of 4.5 during isoelectric focusing. The pure 134 kDa protein was able to increase the specific conductance of artificial lipid bilayer membranes from phosphatidylcholine–phosphatidylserine mixtures by the formation of ion-permeable channels. The channels had an average single-channel conductance of 5.5 nS in 1 M KCl and were found to be cation-selective. Asymmetric addition of the 134 kDa protein to lipid bilayer membranes resulted in an asymmetric voltage-dependence. The analysis of the single-channel conductance as a function of cation radii using the Renkin correction factor and the effect of negative charges on channel conductance suggested that the diameter of the cell wall porin is about 1.0 nm. The channel characteristics of the cell wall channel of *N. corynebacteroides* were compared with those of other members of the mycolata. They share common features because they are composed of small molecular mass subunits and form large and water-filled channels.

Keywords: Cell wall channel; Mycolic acid; Porin; Lipid bilayer membrane; *Nocardia corynebacteroides*

1. Introduction

Nocardia corynebacteroides and other nocardiae belong to the broad and diverse group of the mycolata, the mycolic acid containing actinomycetes [1]. The strain *N. corynebacteroides* ATCC 14898 has been reclassified from *Corynebacterium rubrum* [2,3]. Its correct phylogenetic position within the genus *Nocardia* or *Rhodococcus* has been a matter of debate but it is still within the genus *Nocardia* [4,5]. It is a Gram-positive, strictly aerobic and non-pathogenic bacterium, which is mainly found in soil and water [2]. The vermilion growth of *N. corynebacteroides* occurs regularly in tap-water systems, because of the high resistance of the bacteria against free chloride (0.3–0.6 mg/l) and the existence of a lipid and fat storage system by remarkable formation of vacuoles [3]. *N. corynebacteroides* is used as a substitute of *Mycobacterium tuberculosis* to identify the responsi-

* Corresponding author. Fax: +49-931-888-4509; E-mail: riess@biozentrum.uni-wuerzburg.de

0005-2736/00/$ – see front matter
PII: S0005-2736(00)00332-1

ble antigen and the mechanism in adjuvant arthritis. This means that it contributes to the understanding of this disease, which shares some features common with rheumatoid arthritis of man [6,7]. Thus *N. corynebacteroides* may provide clues to the etiology of human arthritis [8].

In contrast to the most pathogenic *Nocardia* species, *N. corynebacteroides* does not exhibit a pronounced natural resistance to various antimicrobial drugs [9–11], but owns rather a broad sensitivity against antibiotics [2]. It possesses a primarily increased resistance against disinfectant solution of dosing apparatuses [12,13]. Members of the genus *Nocardia* have a thick peptidoglycan layer and large amounts of lipids in the form of mycolic acids in their cell walls [14–18]. Ester bonds connect the 2-branched, 3-hydroxylated fatty acids with the arabinogalactan which is attached to the murein of the cell wall [19–21]. The chain length of these acids varies between 46 and 58 carbon atoms in *Nocardia* [22]. The permeability of the cell wall of certain mycolata is unusually low [23] presumably because the mycolic acid layer represents a second permeability barrier besides the cytoplasmic membrane [24,25].

When the lipid layer on the surface of the mycolata represents a permeability barrier for hydrophilic compounds, the question arises how these substances permeate across this barrier. Cell wall channels have been identified to exist in two pathogenic *Nocardia* strains [26,27] and in other members of the mycolata, such as Mycobacteria [28–30], Corynebacteria [31] and *Rhodococcus* [32]. These channels are wide, water-filled and contain negative point charges. In this study, we extended the search for cell wall channels to another *Nocardia* strain to investigate the question whether pathogenic and non-pathogenic strains contain similar properties concerning the transport of nutrients and hydrophilic compounds through the cell wall. Using lipid bilayer experiments, we could demonstrate that the permeability pathway in the cell wall of *N. corynebacteroides* consists of a channel-forming oligomer, which has a molecular mass of 134 kDa. The monomer has a molecular mass of 23 kDa. The cell wall channel of *N. corynebacteroides* is wide and water-filled. It forces the permeation of cations, which is caused by the presence of negatively charged groups at the channel mouth.

2. Materials and methods

2.1. Bacterial strain and growth conditions

N. corynebacteroides (ATCC 14898) as obtained from the German Collection of Microorganisms and Cell Cultures (DSMZ) was used in all the experiments. The strain was grown in 500 ml Erlenmeyer flasks containing 250 ml *Corynebacterium* media (Media 53/DSMZ) at 30 ± 1°C using a New Brunswick shaker at 120 rpm for 1–2 days. The cell culture was checked for purity and the cells were harvested by centrifugation at 12 000 rpm for 10 min at 4°C.

2.2. Isolation of the channel-forming activity from whole cells using detergents

The cells were treated several times by the freeze and thaw method, which means that the cells were incubated at −80°C and subsequently warmed at 30 ± 2°C. This method was used to break the cells and to separate the cell wall from the cytoplasm. For the extraction of the channel-forming protein, cell walls from about 2 g cell material (wet weight) were treated with two different washing steps. In the first isolation step, the pellet was washed with 10 ml 0.2% SDS+10 mM Tris–HCl, pH 8.0 (buffer I) for 20 h at 50°C under agitation followed by centrifugation at 14 600 × *g* in a Beckman J2-21 M/E centrifuge (rotor JA20) for 10 min. The resulting pellet was then suspended in 10 ml 1% Genapol+10 mM Tris–HCl, pH 8.0 (buffer II) for 20 h at 50°C under agitation and also followed by centrifugation. The channel-forming activity was preferentially present in the final supernatant.

2.3. Two-dimensional (2-D) gel electrophoresis

The first dimension separations were performed as acidic isoelectrofocusing (IEF; 3.5 h at 750 V) in 7.5 mm × 2 mm 4% polyacrylamide gels containing 2% ampholines (1.6% Bio-Lyte 5/7 ampholyte (Bio-Rad, Richmond, CA, USA); 0.4% Bio-Lyte 3/10 ampholyte (Bio-Rad)). The IEF gels were immersed in a solution containing 0.06 M Tris (pH 6.8), 2.3% SDS, 5% β-mercaptoethanol, 10% glycerol and 0.01% bromophenol blue and incubated for 10 min at room temperature before applying to the second SDS–

polyacrylamide dimension. Second-dimensional separations were carried out on a Protean II 2-D Cell (Bio-Rad) at room temperature, on homogeneous running mini-slab gels without stacking gel.

2.4. SDS–PAGE

Analytical and preparative SDS–PAGE was performed according to Laemmli [33]. The gels were stained with Coomassie brilliant blue, Colloidal Coomassie blue [34] or with silver [35].

2.5. Reconstitution experiments with lipid bilayer membranes

The methods used for the lipid bilayer experiments have been described previously in detail [36]. Black lipid bilayer membranes were obtained by painting onto the hole a 1% solution of a mixture (molar ratio 4:1) of diphytanoyl phosphatidylcholine (PC) and phosphatidylserine (PS) (Avanti Polar Lipids, Alabaster, AL, USA) in *n*-decane. The temperature was maintained at 20°C during all experiments. All salts were obtained from Merck (Darmstadt, Germany, analytical grade). Zero-current membrane potential measurements were performed by establishing a salt gradient across membranes containing 100–1000 cell wall porins as it has been described earlier [37] using a high impedance electrometer (Keithley 617).

2.6. Estimation of the channel diameter using the Renkin correction factor

The calculation of the channel size is possible from the single-channel conductance data when only cations or anions can permeate through the channel and when the ions move inside a wide, water-filled channel [30]. Then the entry of the ions in the channel is the rate-limiting step and the Renkin correction factor may be used to estimate the channel size from the relative permeability of the different ions as has been shown previously [30,38]. Using this method, the relative conductance of the different ions with respect to Rb^+ is given as a function of the hydrated ion radius, which corresponds to the dependence of the relative rate of permeation on solute radii in the liposome swelling assay with solutes of different size [39].

2.7. Effect of negatively charged groups attached to the channel mouth

Negative charges at the pore mouth result in a substantial ionic strength-dependent surface potential at the pore mouth that attracts cations and repels anions. Accordingly, they influence both single-channel conductance and zero-current membrane potential. A quantitative description of the effect of the point charges on the single-channel conductance has been given in previous studies [29,40–42]. The same formalism was also used here for the calculation of the effective channel radius and the number of negatively charged point charges attached to the channel mouth.

3. Results

3.1. Isolation, purification and pI of the channel-forming protein from the cell wall

For the isolation of the channel-forming protein, we treated the bacterial pellet with the frost and defrost method, which is a standard method for cell fractionation of Gram-negative bacteria. In this step, we broke the cells and therefore we could remove most of the soluble cell components with the

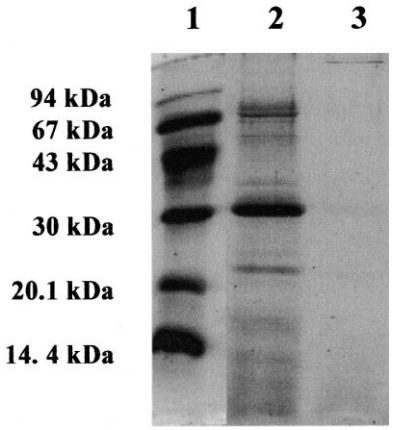

Fig. 1. 12% SDS–PAGE of different purification steps of the cell wall channel of *N. corynebacteroides*. Lane 1: Molecular mass markers 94 kDa, 67 kDa, 43 kDa, 30 kDa, 20.1 kDa and 14.4 kDa. Lane 2: 15 μl of the supernatant of step I was solubilized at 40°C for 30 min in 5 μl sample buffer. Lane 3: 15 μl of the supernatant of step II was solubilized at 40°C for 30 min in 5 μl sample buffer. Coomassie blue staining.

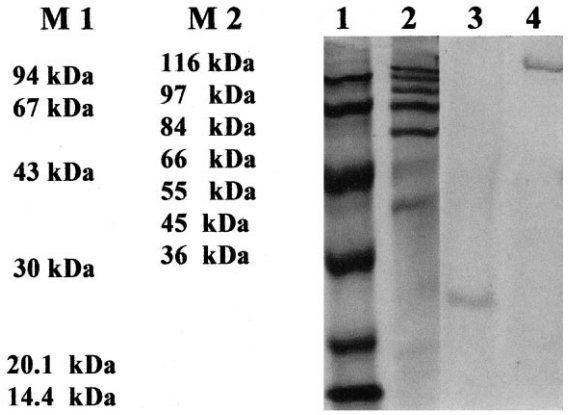

Fig. 2. 12% SDS–PAGE of pure cell wall channel protein of *N. corynebacteroides* obtained by elution of the 134 kDa band from preparative SDS–PAGE. Lane 1: Molecular mass markers 94 kDa, 67 kDa, 43 kDa, 30 kDa, 20.1 kDa and 14.4 kDa. Lane 2: Molecular mass markers 205 kDa, 116 kDa, 97 kDa, 84 kDa, 66 kDa, 55 kDa, 45 kDa and 36 kDa. Lane 3: 3 μg of the pure protein was solubilized at 100°C for 15 min in 10 μl sample buffer and 10 μl distilled water. Lane 4: 3 μg of the pure protein was solubilized at 40°C for 30 min in 10 μl sample buffer and 10 μl distilled water. Colloidal Coomassie blue staining [34].

subsequent washing steps. This washing procedure in a modified manner has successfully been used in previous studies of the cell wall channels of *Nocardia farcinica* and *Nocardia asteroides* [26,27]. The channel-forming activity was preferentially present in the final supernatant. SDS–PAGE of the corresponding proteins demonstrated that it contained a major protein band with an apparent molecular mass of about 134 kDa (see Fig. 1).

Further purification of the channel-forming protein was achieved by excision of this band from preparative SDS–PAGE and its extraction with 500 μl 1% Genapol, 10 mM Tris–HCl, pH 8 (see Fig. 2). Addition of the extract to a planar lipid bilayer resulted in a very fast reconstitution of channels. When different molecular mass regions were excised from the same SDS–PAGE, highest channel-forming activity was observed for the 134 kDa band. However, we observed also that a small channel-forming activity was smeared across the whole molecular mass region between about 22 and 134 kDa. This result indicated that the 134 kDa band may represent the channel-forming oligomer. This was confirmed by SDS–PAGE when the 134 kDa protein band was heated to 100°C for 10 min in sample buffer. The gel showed that the 134 kDa band was composed of one subunit with a molecular mass of about 23 kDa (see Fig. 2). The protein focused at a p*I* of 4.5 (data not shown) during isoelectric focusing using a preparatory 2-D electrophoresis method.

3.2. *Effect of the cell wall protein on the conductance of lipid bilayer membranes*

We performed conductance measurements with lipid bilayer membranes to study the interaction of the cell wall porin with artificial membranes. Membranes were formed from 1% PC/PS mixtures (molar ratio 4:1) dissolved in *n*-decane. The addition of the 134 kDa cell wall protein in small concentration (100 ng/ml) to one or both sides of the lipid membranes resulted in a strong increase of the conductance within 30 min by several orders of magnitude above that of those of membranes without the protein (from about 0.05 μS/cm^2 to 150 μS/cm^2). Only a small further increase (as compared with the initial

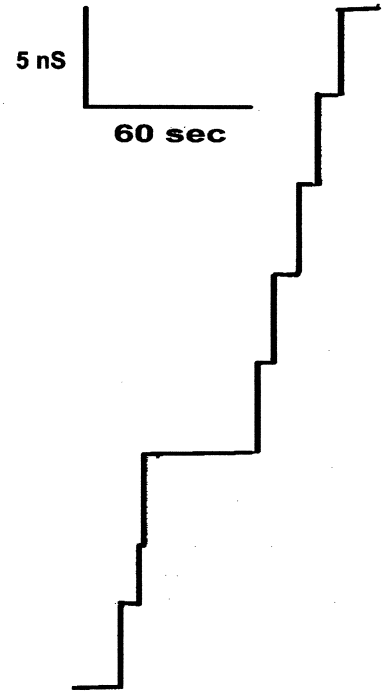

Fig. 3. Single-channel recording of a PC/PS (molar ratio 4:1)/*n*-decane membrane in the presence of the 134 kDa protein from the cell wall of *N. corynebacteroides*. The aqueous phase contained 1 M KCl and 10 mM Tris–HCl, pH 8 and 10 ng/ml cell wall protein. The applied membrane potential was 10 mV; $T = 20$°C.

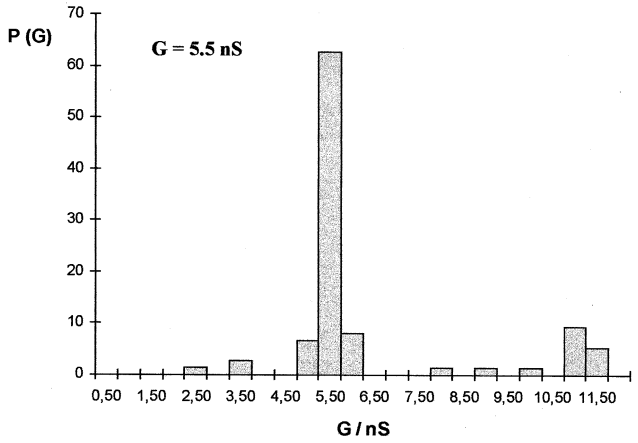

Fig. 4. Histogram of the probability $P(G)$ for the occurrence of a given conductivity unit observed with membranes formed of PC/PS (molar ratio 4:1)/*n*-decane in the presence of the cell wall protein of *N. corynebacteroides*. $P(G)$ is the probability that a given conductance increment G is observed in the single-channel experiments. It was calculated by dividing the number of fluctuations with a given conductance increment by the total number of conductance fluctuations. The aqueous phase contained 1 M KCl and 10 mM Tris–HCl, pH 8. The applied membrane potential was 10 mV; $T = 20°C$. The average single-channel conductance was 5.5 nS for 57 single-channel events (right-hand maximum).

one) occurred after that time. Control experiments with Genapol alone at the same concentration as in the experiments with protein demonstrated that the membrane activity was caused by the presence of the cell wall protein and not by the detergent.

3.3. Single-channel analysis

The addition of smaller concentrations of the cell wall porin protein (10 ng/ml) to PC/PS/*n*-decane membranes allowed the resolution of stepwise conductance increases. Fig. 3 shows a single-channel recording 5 min after the addition of the cell wall porin to a lipid bilayer membrane. The current increased in step-like fashion and had a long lifetime (mean lifetime more than 5 min). Fig. 4 shows a histogram of the conductance fluctuations observed under the conditions of Fig. 3 (10 mV membrane potential, 1 M KCl, 10 mM Tris–HCl, pH 8). The major conductance step was about 5.5 nS but sometimes also smaller channels were observed. For larger voltages across the membranes, the histogram of the conductance fluctuations became more complicated because some additional conductance levels occurred. In particular, the cell wall porin switched to different substates that were not observed at 10 mV (see below). These results suggested that the cell wall porin of *N. corynebacteroides* was voltage-dependent for voltages above 20 mV.

3.4. Size of the cell wall channel

Further single-channel experiments were performed to get some insight in the biophysical properties of the cell wall porin of *N. corynebacteroides*. The results show that cations had a substantial influence on the single-channel conductance (see Table 1). This result is consistent with the assumption that the cell wall channel is cation-selective. The conductance of cations followed the series $Rb^+ > Cs^+ > K^+ \approx NH_4^+ > Na^+ > Li^+ > N(CH_3)_4^+ > N(C_2H_5)_4^+ = Tris^+$, which means that it followed approximately their mobility sequence in the aqueous phase. This result suggests that the cell wall porin is a wide channel, which has inside only a small field strength and no selectivity filter (i.e. no binding site). Table 1 shows

Table 1
Average single-channel conductance, G, of the cell wall channel of *N. corynebacteroides* in different salt solutions[a]

Salt	Concentration (M)	G (nS)
LiCl	1.0	2.50
NaCl	1.0	2.75
KCl	0.01	0.60
	0.03	0.80
	0.05	1.00
	0.10	1.20
	0.3	2.10
	0.5	3.50
	1.0	5.50
	3.0	13.20
KCH_3COO	1.0	4.50
RbCl	1.0	6.50
CsCl	1.0	6.00
NH_4Cl	1.0	5.50
$N(CH_3)_4Cl$	1.0	1.75
$N(C_2H_5)_4Cl$	1.0	0.95
Tris–Cl	1.0	0.95

[a]The membranes were formed of PC/PS (molar ratio 4:1) dissolved in *n*-decane. The aqueous solutions were buffered with 10 mM Tris–HCl and had a pH of 8 unless otherwise indicated. The applied voltage was 10 mV, and the temperature was 20°C. The average single-channel conductance, G, was calculated from at least 80 single events from the right-hand maxima of the histograms.

also the average single-channel conductance, G, as a function of the KCl concentration in the aqueous phase. Measurements were performed down to 0.01 M KCl. Similar to the conditions with other cell wall porins [28,29,31], we did not observe a 1:1 relationship between single-channel conductance and KCl concentration, which would be expected for wide water-filled channels similar to those formed by general diffusion porins of Gram-negative bacteria [43,44].

3.5. Selectivity of the cell wall porin of N. corynebacteroides

Zero-current membrane potential measurements were carried out to obtain further information about the structure of the *N. corynebacteroides* cell wall porin. After the incorporation of 100–1000 channels into the PC/PS membranes, the salt concentration on one side of the membranes was raised 5-fold beginning from 100 mM and the zero-current potential was measured 5 min after every increase of the salt gradient across the membrane. For all three salts (KCl, LiCl, KCH_3COO) employed in these experiments, the more dilute side of the membrane (100 mM versus 500 mM) became always positive, which indicated preferential movement of the cations through the channel, i.e. the cell wall porin is weakly cation-selective as was already suggested from the single-channel recordings. The zero-current membrane potential for the salts mentioned above had values of 17 mV (LiCl), 21 mV (KCl) and 25 mV (potassium acetate). Analysis of these potentials using the Goldman–Hodgkin–Katz equation [37] suggested that anions also could have a certain permeability through the channel because the ratios of the permeability P_{cation} and P_{anion} were 2.8 (LiCl), 3.8 (KCl), and 5.0 (potassium acetate).

3.6. The cell wall channel porin of N. corynebacteroides is voltage-dependent in a defined asymmetric manner

In single-channel recordings, the cell wall porin exhibited some flickering at higher voltages, i.e. it showed rapid transitions between open and closed configurations. This could be caused by voltage-dependent closing of the channels (Fig. 5). The channel-forming protein was added in a concentration of 500 ng/ml to one side of a black PC/PS/*n*-decane membrane (to the *cis*-side). After 30 min, the conductance had increased considerably. At this point, we applied different potentials to the membrane. We applied first +60 mV (upper trace of Fig. 5) and then −60 mV to the *cis*-side of the membrane (lower trace of Fig. 5). Then we repeated the experiment with 70 and 80 mV. In all cases, we observed a decrease of the membrane current in an exponential manner.

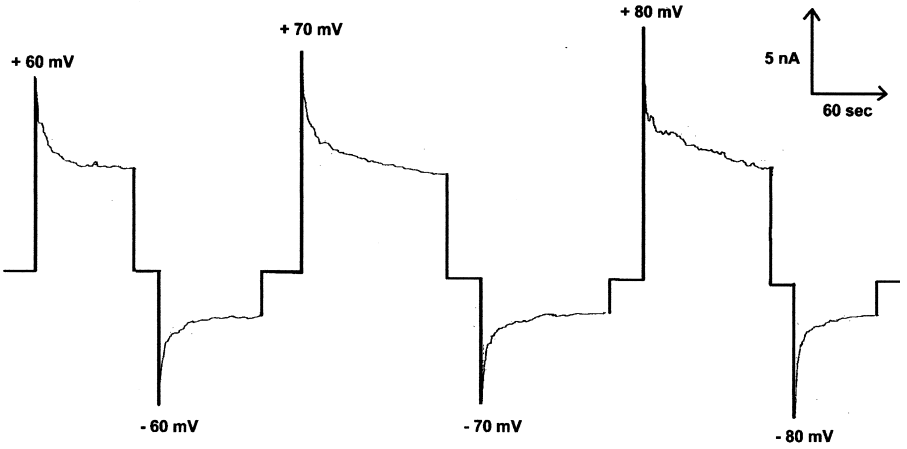

Fig. 5. Study of the voltage-dependence of *N. corynebacteroides* porin. 500 ng/ml of the cell wall channel protein was added to the *cis*-side of a PC/PS (molar ratio 4:1)/*n*-decane membrane and the reconstitution of the channels was followed for about 30 min. When about 90 channels were reconstituted into the membrane, increasing positive (upper traces) and negative voltages (lower traces) were applied to the *cis*-side of the membrane and the membrane current was measured as a function of the time. The aqueous phase contained 1 M KCl and 10 mM Tris–HCl, pH 8; $T = 20°C$.

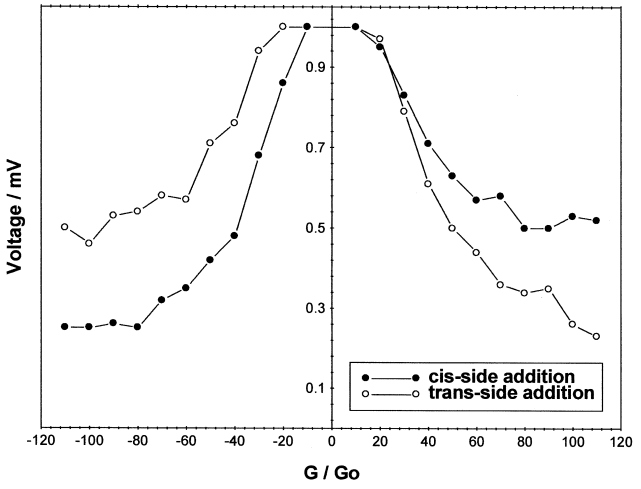

Fig. 6. Ratio of the conductance G at a given membrane potential (V_m) divided by the conductance G_o at 10 mV as a function of the membrane potential V_m. The open circles indicate the measurements in which *N. corynebacteroides* porin was added to the *trans*-side of a membrane; the closed circles measurements in which the porin was added to the *cis*-side of membranes. The membrane potential refers always to the *cis*-side of the membrane. The aqueous phase contained 1 M KCl, 10 mM Tris–HCl, pH 8.0 and 100 ng/ml porin. The membranes were formed from PC/PS (molar ratio 4:1) dissolved in *n*-decane. $T = 20°C$.

Surprisingly, we noticed a weak asymmetry in response to the voltage depending on the sideness of voltage application and protein addition. For negative potential at the *cis*-side, 50% of the channels closed at a membrane potential V_o of −35 mV, whereas 70 mV was needed for the closing of 50% of the channels when the *cis*-side was positive. This result indicated asymmetric insertion of the cell wall porin into the membranes.

The data of the experiment of Fig. 5 and similar experiments were analyzed in the following way: the membrane conductance (G) as a function of voltage, V_m, was measured when the opening and closing of channels reached an equilibrium, i.e. after the exponential decay of the membrane current following the voltage step V_m. G was divided by the initial value of the conductance (G_o, which was a linear function of the voltage) obtained immediately after the onset of the voltage. The data of Fig. 6 (open and closed circles) correspond to the asymmetric voltage-dependence of the cell wall porin (mean of four membranes) when the protein was added to the *cis*-side (closed circles) or to the *trans*-side (open circles). To study the voltage-dependence in more detail, the data of Fig. 6 were analyzed assuming a Boltzmann distribution between the number of open and closed channels, N_o and N_c, respectively [45]:

$$N_o/N_c = \exp(nF(V_m - V_o)/RT) \quad (1)$$

F, R and T are Faraday's constant, gas constant and absolute temperature, respectively, n is the number of charges moving through the entire transmembrane potential gradient for channel gating and V_o is the potential at which 50% of the total number of channels are in the closed configuration. The open-to-closed ratio of the channels, N_o/N_c, may be calculated from the data in Fig. 6 according to

$$N_o/N_c = (G - G_{min})/G_o - G) \quad (2)$$

G is in this equation the conductance at a given membrane potential V_m, G_o and G_{min} are the conductances at 10 mV (conductance of the open state) and very high voltages, respectively. The semilogarithmic plot of the ratio N_o/N_c as a function of the transmembrane V_m could be fitted to straight lines (not shown). The lines can be used for the calculation of the number of gating charges n (number of charges involved in the gating process) and the midpoint potential V_o (potential at which the number of open and closed channels is identical). The midpoint potential of the distribution of open and closed channels was −35 mV for the addition of the cell wall porin to the *cis*-side, the midpoint potential for the addition of the cell wall porin to the *trans*-side was 32 mV. The gating charge was in both cases close to 1.44.

4. Discussion

4.1. The cell wall of N. corynebacteroides contains a channel-forming protein

The results presented here demonstrate that the cell wall of the non-pathogenic strain *N. corynebacteroides* contains a channel, which has presumably the same function as Gram-negative bacterial porins [36,43,46]. Its characteristics are similar to those of other Gram-positive bacteria, such as *Mycobacterium chelonae* [28,29], *Rhodococcus erythropolis* [32] and *Corynebacterium glutamicum* [31]. The common

structural element of all these bacteria is besides the thick peptidoglycan layer the large amount of lipids in form of mycolic acids. This mycolic acid layer acts as a permeability barrier toward hydrophilic compounds [14,15,17,18] in a similar way as the outer membrane of Gram-negative bacteria. Water-filled channels are needed to overcome these permeability barriers. The cell wall porin of *N. corynebacteroides* was purified to homogeneity using preparative SDS–PAGE and has a molecular mass of about 134 kDa. Upon heating, the protein dissociated into one subunit of a molecular mass of about 23 kDa on SDS–PAGE. This means that the channel is composed of subunits similar to the situation in *Mycobacterium smegmatis*, where the 3 nm wide channel is also formed by a small subunit (19 kDa) [27,30]. Furthermore, these subunits agree in the p*I* (*N. corynebacteroides*: p*I* 4.5; *M. smegmatis*: p*I* 4.49).

The 23 kDa subunit of the cell wall channel had obviously a high aggregation tendency, because we were able to detect channels when we eluted molecular mass bands higher than 23 kDa from preparative SDS–PAGE although the channel-forming activity was much smaller in these cases as compared with that of the 134 kDa oligomer. This result confirms that the channel is formed by a protein oligomer. Furthermore, it seems to be impossible that a protein of 23 kDa alone forms such a wide water-filled channel. It is noteworthy that these results are in contrast to those from the pathogenic *Nocardia* strains we have previously investigated [26,27]. The cell wall channels of both, *N. farcinica* and *N. asteroides*, consist of two subunits of different molecular masses. Interestingly, the cell wall channel of *R. erythropolis* consists also of only one subunit [32].

4.2. Evaluation of the diameter of the cell wall channel of N. corynebacteroides

The diameter of the channel of *N. corynebacteroides* was calculated on the basis of its single-channel conductance [30]. It is based on the same assumptions, which have been used previously for the derivation of the Renkin equation [38] for the diffusion of neutral molecules through porous membranes (see Section 2). Fig. 7 shows the fit of the single-channel conductance of the porin channel from *N. corynebacteroides* with the Renkin equation (equation 1 of [30]) times the aqueous diffusion coefficient of the ions. The data are given relative to the data for Rb^+ ($a = 0.105$ nm), which were set to unity and the best fit of the single-channel conductance was obtained with $r = 1.0$ nm (diameter 2.0 nm). The pore diameter is similar to those found for the porins of *R. erythropolis* [32] and *C. glutamicum* [31].

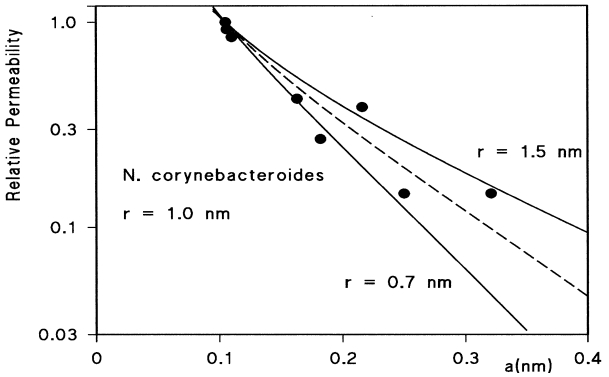

Fig. 7. Fit of the single-channel conductance data of the *N. corynebacteroides* cell wall channel by using the Renkin correction factor times the aqueous diffusion coefficients of the different cations [30]. The product of both numbers was normalized to 1 for $a = 0.105$ nm (Rb^+). Single-channel conductances were normalized to the ones of Rb^+ and plotted versus the hydrated ion radii taken from table 2 of [30]. The closed points correspond to Li^+, Na^+, K^+, NH_4^+, Cs^+, $N(CH_3)_4^+$, $N(C_2H_5)_4^+$ and $Tris^+$, which were all used for the pore diameter estimation (see Section 4). The fit (solid lines) is shown for $r = 1.5$ nm (upper line) and $r = 0.7$ nm (lower line). The best fit was achieved with $r = 1.0$ nm (diameter = 2.0 nm), which corresponds to the broken line.

4.3. Ion selectivity of the N. corynebacteroides cell wall porin

The single-channel conductance was not saturable at high salt concentration, and the conductance was not a linear function of the bulk aqueous concentration (see Table 1). This means (i) that the cation specificity is not related to the presence of a binding site inside the channel and (ii) that there is some indication for the influence of point charges on the ion selectivity. When we apply a similar treatment to the *N. corynebacteroides* channel as was previously proposed for other cell wall channels, we receive also a reasonable fit of the concentration-dependence of the single-channel conductance by using equations 1–3 of [29], assuming that the channel has a diameter

of 2.2 nm ($r = 1.1$ nm) and that 2.7 point charges ($= 2.5 \cdot 10^{-19}$ As) are attached to the channel mouth. The results of this fit are enclosed in Fig. 8. Taken together with the diameter derived above from the relative permeability of different ions, it demonstrates that the cell wall channel of *N. corynebacteroides* has a larger diameter than the pathogenic *Nocardia* strains ($d = 1.5$ nm) [26,27], which is in agreement with a higher susceptibility for all antibiotics [2,47].

4.4. The N. corynebacteroides cell wall porin is voltage-dependent

Experiments with higher membrane potentials suggested that the *N. corynebacteroides* cell wall porin is voltage-dependent in a defined asymmetric manner. The channel starts to close with a voltage of about ± 30 mV and reaches a maximum closure of about ± 100 mV. This result indicated 100% orientation of the channel reconstituted into the lipid bilayer membrane. When we assume that in vivo the *cis*-side of the mycolic acid layer is exposed to the cytoplasmic membrane, this observation could mean that a negative potential at the inner side of the cell wall could regulate its permeability. So far it is rather unlikely that this potential could be the result of an ionic gradient because of the high permeability of the cell wall porin for ions. However, the situation in the gap between the cytoplasmic membrane and the mycolic acid layer could be similar as in the periplasmic space of Gram-negative bacteria, which means that a Donnan potential could exist because of the distribution of charged molecules [48]. Our results suggest that this Donnan potential could lead to voltage-dependent control of the cell wall permeability of *N. corynebacteroides*.

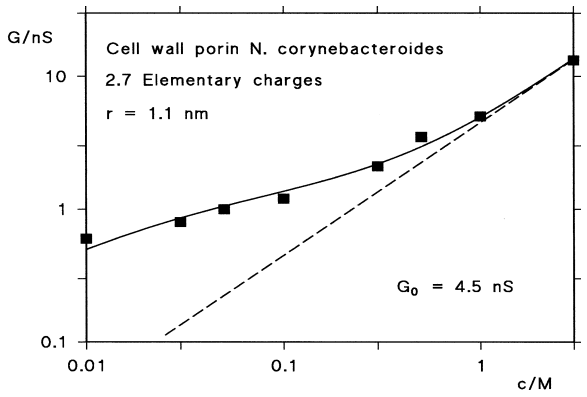

Fig. 8. Single-channel conductance of the cell wall channel of *N. corynebacteroides* as a function of the KCl concentration in the aqueous phase (full squares). The solid line represents the fit of the single-channel conductance data with the Nelson and McQuarrie [40] formalism (equations 1–3 of [29]) assuming the presence of negative point charges (2.7 negative charges; $q = -4.3 \cdot 10^{-19}$ As) at the channel mouth and assuming a channel diameter of 2.2 nm. *c*, concentration of the KCl solution in M (molar); *G*, average single-channel conductance in nS (nano Siemens, 10^{-9} S). The broken (straight) line shows the single-channel conductance of the cell wall channel in the absence of point charges and corresponds to a linear function between channel conductance and bulk aqueous concentration. The single-channel conductance in the absence of negative point charges is 4.5 nS at 1 M KCl.

4.5. Implications for the permeability of the cell wall

The non-pathogenic strain *N. corynebacteroides* is susceptible to most common antibiotics similar to the

Table 2
Comparison of the cell wall channel properties of *N. corynebacteroides*, *N. farcinica*, *M. chelonae*, *R. erythropolis* and *C. glutamicum*

Cell wall porin	G (nS) in 1 M KCl	Selectivity P_c/P_a in KCl	Negative point charges at the channel mouth	Channel diameter (nm)	Ref.
N. corynebacteroides	5.5	3.8	2.7	2.0[b], 2.2[c]	this study
N. farcinica	3.0	8.2	1.3	1.4[b], 1.6[c]	[26]
M. chelonae	2.7	14.0	2.5	2.2[a], 2.0[c]	[28,29]
R. erythropolis	6.0	11.8	2.7	2.0[a,b]	[32]
C. glutamicum	5.5	8.1	2.0	2.2[b,c]	[31]

[a]The channel diameter was estimated from the liposome swelling assay.
[b]The channel diameter was estimated from the single-channel conductance as a function of the hydrated ion radii.
[c]The channel diameter was estimated from the effect of negative point charges on single-channel conductance.

situation within the genus *Rhodococcus*, which exhibit a broad sensitivity against antimicrobial reagents besides β-lactam antibiotics and in contrast to the pathogenic strain *N. farcinica* which is highly resistant to antibiotics [10,47]. *N. farcinica* has some susceptibility against the positively charged antibiotics where the sulfonamide sulfodiazine is particularly effective against nocardiosis [10]. These observations tend to agree with the cation selectivity of the cell wall porin, although the permeability of the cell wall of *N. farcinica* for different antibiotics is not known. Negative point charges attached to the cell wall porin could favor the permeation of positively charged antibiotics. Similar effects have been observed for *M. smegmatis* where negatively charged cephalosporins had a 10–20-fold lower permeability through the cell wall than the zwitterionic cephaloridine [30], and for the mycobacterial porin in *M. chelonae* [23,29]. The fact that the cell wall channel of *N. corynebacteroides* owns a larger diameter, is not as cation-selective and not as voltage-dependent as the other two pathogenic *Nocardia* strains we already investigated, allows to understand its sensitivity to different charged antibiotics. Furthermore, the channel allows the permeation of higher molecular mass substrates than the pathogenic *Nocardia* strains. It consists of only one subunit, which leads to a novel channel architecture in the genus *Nocardia*, although the correct phylogenetic classification of *N. corynebacteroides* is still a matter of debate [4,5].

It is noteworthy that the cell wall porin of *N. corynebacteroides* had properties similar to those found in the cell walls of distantly related other actinomycetes. All have negative charges at the channel mouth and similar diameters of the channel as Table 2 clearly indicates. These properties seem to be a feature that has been conserved in the cell wall porins of bacteria in the suborder *Corynebacterineae* of the order *Actinomycetales* that belongs to the subclass *Actinobacteridae* of the class *Actinobacteria*.

Acknowledgements

This investigation was supported by a Grant of the Deutsche Forschungsgemeinschaft (project Be 865/9) and the Fonds der Chemischen Industrie.

References

[1] E. Stackebrandt, F.A. Rainey, N.L. Ward-Rainey, Proposal for a new hierarchic classification system *Actinobacteria classis* nov., Int. J. Syst. Bacteriol. 47 (1997) 479–491.
[2] J.A. Serrano, R.V. Tablante, A.A. de Serrano, G.C. de San Blas, T. Imaeda, Physiological, chemical and ultrastructural characteristics of *Corynebacterium rubrum*, J. Gen. Microbiol. 70/2 (1972) 339–349.
[3] W. Graf, L. Bauer, Red bacterial growth (*Corynebacterium rubrum* n. spec.) in tap water systems, Zent.bl. Bakteriol. [Orig B] 157/4 (1973) 291–303.
[4] M. Goodfellow, Genus *Rhodococcus*, in: P.H.A. Sneath, N.S. Mair, M.E. Sharpe and J.G. Holt (Eds.), Bergey's Manual of Systematic Bacteriology, Vol. 2, William and Wilkins, Baltimore, MD, 1986, pp. 1472–1481.
[5] F.A. Rainey, J. Burghardt, R.M. Kroppenstedt, S. Klatte, E. Stackebrandt, Phylogenetic analysis of the genera *Rhododdcoccus* and *Nocardia* and evidence for the evolutionary origin of the genus *Nocardia* from within the radiation of *Rhodococcus* species, Microbiology 141 (1995) 523–528.
[6] F. Paronetto, Adjuvant arthritis induced by *Corynebacterium rubrum*, Proc. Soc. Exp. Biol. Med. 133/1 (1970) 296–298.
[7] F. Paronetto, Studies on experimental arthritis induced by *Corynebacterium rubrum*. 1. Localization of the arthritogenic factor in the cell walls, Arthritis Rheum. 15/1 (1972) 36–40.
[8] J.C. Lorentzen, Identification of arthritogenic adjuvants of self and foreign origin, Scand. J. Immunol. 49/1 (1999) 45–50.
[9] P. Boiron, F. Provost, G. Chevrier, B. Dupont, Review of nocardial infections in France 1987 to 1990, Eur. J. Clin. Microbiol. Infect. Dis. 11 (1992) 709–714.
[10] K.P. Schaal, W. Leischik, Zur Antibiotikatherapie der Nocardiose, Dtsch. Med. Wschr. 94 (1969) 2505–2507.
[11] K.P. Schaal, H. Schütt-Gerowitt and A. Goldmann, In vitro and in vivo studies on the efficacy of various antimicrobial agents in the treatment of human nocardiosis, in: G. Szabo, S. Biro and M. Goodfellow (Eds.), Biological, Biochemical, and Biomedical Aspects of Actinomycetes, Academiai Kiado, Budapest, 1986, pp. 619–633.
[12] M. Heinzel, H. Bellinger, Microbiological investigations with decentral dosing apparatuses for disinfectants. Part 1: Investigations of cell number, Zent.bl. Bakteriol. Mikrobiol. Hyg. [B] 174/1 (1981) 299–313.
[13] M. Heinzel, H. Bellinger, Microbiological investigations with decentral dosing apparatuses for disinfectants. Part 2: Resistance behaviour of isolated bacteria, Zent.bl. Bakteriol. Mikrobiol. Hyg. [B] 176/1 (1982) 47–54.
[14] L. Barksdale, The genus *Corynebacterium*, in: M.P. Starr, H. Stoll, H.G. Trüper, A. Balows and H.G. Schlegel (Eds.), The Prokaryotes, Vol. 1, Springer, Berlin, 1981, pp. 1827–1837.
[15] M. Goodfellow, M.D. Collins, D.E. Minnikin, Thin-layer chromatographic analysis of mycolic acid and other long-chain components in whole organism methanolysates of coryneform and related taxa, J. Gen. Microbiol. 96 (1976) 351–358.

[16] M. Goodfellow, D.E. Minikin, Nocardioform bacteria, Ann. Rev. Microbiol. 33 (1977) 159–180.
[17] K. Ochi, Phylogenetic analysis of mycolic acid-containing wall-chemotype IV actinomycetes and allied taxa by partial sequencing of ribosomal protein AT-L30, Int. J. Syst. Bacteriol. 45 (1995) 653–660.
[18] J. Liu, C.E. Barry III, G.S. Besra, H. Nikaido, Mycolic acid structure determines the fluidity of the mycobacterial cell wall, J. Biol. Chem. 271 (1996) 29545–29551.
[19] D.E. Minnikin, Lipids: Complex lipids, their chemistry, biosynthesis and roles, in: C. Ratledge and J.C. Stanford (Eds.), The Biology of the Mycobacteria, Academic Press, New York, 1982, pp. 95–184.
[20] D.E. Minnikin, Chemical targets in cell envelopes, in: M. Hopper (Ed.), Chemotherapy of Tropical Diseases, John Wiley and Sons Ltd., Chichester, 1987, pp. 19–43.
[21] D. Chatterjee, C.M. Bozic, M. McNeil, P.J. Brennan, Structural features of the arabinan component of the lipoarabinomannan of *Mycobacterium tuberculosis*, J. Biol. Chem. 266 (1991) 9652–9660.
[22] J.G. Holt, N.R. Krieg, P.H.A. Sneath, J.T. Staley and S.T. Williams, Nocardioform actinomycetes, in: Bergey's Manual of Determinative Biology, 9th edn., The Williams and Wilkins Co., Baltimore, MD, 1994, pp. 625–650.
[23] V. Jarlier, H. Nikaido, Permeability barrier to hydrophilic solutes in *Mycobacterium chelonae*, J. Bacteriol. 172 (1990) 1418–1423.
[24] H. Nikaido, S.H. Kim, E.Y. Rosenberg, Physical organisation of lipids in the cell wall of *Mycobacterium chelonae*, Mol. Microbiol. 8 (1993) 1025–1030.
[25] P.J. Brennan, H. Nikaido, The envelope of mycobacteria, Annu. Rev. Biochem. 64 (1995) 29–63.
[26] F.G. Rieß, T. Lichtinger, R. Cseh, A.F. Yassin, K.P. Schaal, R. Benz, The cell wall channel of *Nocardia farcinica*: Biochemical identification of the channel-forming protein and biophysical characterization of the channel properties, Mol. Microbiol. 29 (1998) 139–150.
[27] F.G. Rieß, T. Lichtinger, A.F. Yassin, K.P. Schaal, R. Benz, The cell wall porin of the Gram-positive bacterium *Nocardia asteroides* forms cation-selective channels that exhibit asymmetric voltage-dependence, Arch. Microbiol. 171 (1999) 173–182.
[28] J. Trias, V. Jarlier, R. Benz, Porins in the cell wall of mycobacteria, Science 258 (1992) 1479–1481.
[29] J. Trias, R. Benz, Characterization of the channel formed by the mycobacterial porin of *Mycobacterium chelonae* in lipid-bilayer membranes: demonstration of voltage dependent regulation and the presence of negative point charges at the channel mouth, J. Biol. Chem. 268 (1993) 6234–6240.
[30] J. Trias, R. Benz, Permeability of the cell wall of *Mycobacterium smegmatis*, Mol. Microbiol. 14 (1994) 283–290.
[31] T. Lichtinger, A. Burkovski, M. Niederweis, R. Krämer, R. Benz, Biochemical and biophysical characterization of the cell wall channel of *Corynebacterium glutamicum*: the channel is formed by a low molecular mass subunit, Biochemistry 37 (1998) 15024–15032.
[32] T. Lichtinger, G. Reiss, R. Benz, Biochemical identification and biophysical characterization of a channel-forming protein from *Rhodococcus erythropolis*, J. Bacteriol. 182 (2000) 764–770.
[33] U.K. Laemmli, Cleavage of structural proteins during the assembly of the head of bacteriophage T4, Nature 227 (1970) 680–685.
[34] W. Erhardt, V. Neuhoff, N. Arnold, D. Taube, Improved staining of proteins in polyacrylamide gels including isoelectric focusing gels with clear background at nanogram sensitivity using CBB G-250 und R-250, Electrophoresis 9 (1988) 255–262.
[35] H.J. Gross, H. Baier, H. Blum, Improved silver staining of plant proteins, RNA and DNA in polyacrylamide gels, Electrophoresis 8 (1987) 93–99.
[36] R. Benz, K. Janko, W. Boos, P. Läuger, Formation of large, ion-permeable membrane channels by the matrix protein (porin) of *Escherichia coli*, Biochim. Biophys. Acta 511 (1978) 305–319.
[37] R. Benz, K. Janko, P. Läuger, Ionic selectivity of pores formed by the matrix protein (porin) of *Escherichia coli*, Biochim. Biophys. Acta 551 (1979) 238–247.
[38] E.M. Renkin, Filtration, diffusion, and molecular sieving through porous cellulose membranes, J. Gen. Physiol. 38 (1954) 225–243.
[39] H. Nikaido, E.Y. Rosenberg, Effect of solute size on diffusion rates through the transmembrane pores of the outer membrane of *Escherichia coli*, J. Gen. Physiol. 77 (1981) 121–135.
[40] A.P. Nelson, D.A. McQuarrie, The effect of discrete charges on the electrical properties of the membrane, J. Theor. Biol. 55 (1975) 13–27.
[41] R. Menestrina, R. Antolini, Ion transport through the hemocyanin channels in oxidized cholesterol membranes, Biochim. Biophys. Acta 643 (1981) 616–625.
[42] R. Benz, K.H. Hardie, C. Hughes, Pore formation in artificial membranes by the secreted hemolysins of *Proteus vulgaris* and *Morganella morganii*, Eur. J. Biochem. 220 (1994) 339–347.
[43] R. Benz, Structure and function of porins from Gram-negative bacteria, Ann. Rev. Microbiol. 42 (1988) 359–393.
[44] M.S. Weiss, A. Kreusch, E. Schlitz, U. Nestel, W. Welte, J. Weckesser, G.E. Schultz, The structure of porin from *Rhodobacter capsulatus* at 1.8 Å resolution, FEBS Lett. 280 (1991) 379–382.
[45] O. Ludwig, V. De Pinto, F. Palmieri, R. Benz, Pore formation by the mitochondrial porin of rat brain in lipid bilayer membranes, Biochim. Biophys. Acta 860 (1986) 268–276.
[46] H. Nikaido, M. Vaara, Molecular basis of bacterial outer membrane permeability, Microbiol. Rev. 49 (1985) 1–32.
[47] M.M. McNeil, J.M. Brown, The medically important aerobic actinomycets: epidemology and microbiology, Clin. Microbiol. Rev. 7/3 (1994) 357–417.
[48] K. Sen, J. Hellman, H. Nikaido, Porin channels in intact cells of *Escherichia coli* are not affected by Donnan potentials across the outer membrane, J. Biol. Chem. 263 (1988) 1182–1187.